ARMY RESEARCH LABORATORY

Spall Strength of Tungsten Carbide

by Dattatraya P. Dandekar

ARL-TR-3335 **September 2004**

NOTICES

Disclaimers

The findings in this report are not to be construed as an official Department of the Army position unless so designated by other authorized documents.

Citation of manufacturer's or trade names does not constitute an official endorsement or approval of the use thereof.

Destroy this report when it is no longer needed. Do not return it to the originator.

Army Research Laboratory
Aberdeen Proving Ground, MD 21005-5066

ARL-TR-3335 **September 2004**

Spall Strength of Tungsten Carbide

Dattatraya P. Dandekar
Weapons and Materials Research Directorate, ARL

REPORT DOCUMENTATION PAGE	Form Approved OMB No. 0704-0188

1. REPORT DATE *(DD-MM-YYYY)*	2. REPORT TYPE	3. DATES COVERED (From - To)
September 2004	Final	July 2002–February 2004

4. TITLE AND SUBTITLE
Spall Strength of Tungsten Carbide

5a. CONTRACT NUMBER

5b. GRANT NUMBER

5c. PROGRAM ELEMENT NUMBER

6. AUTHOR(S)
Dattatraya P. Dandekar

5d. PROJECT NUMBER
AH43

5e. TASK NUMBER

5f. WORK UNIT NUMBER

7. PERFORMING ORGANIZATION NAME(S) AND ADDRESS(ES)
U.S. Army Research Laboratory
ATTN: AMSRD-ARL-WM-TD
Aberdeen Proving Ground, MD 21005-5066

8. PERFORMING ORGANIZATION REPORT NUMBER
ARL-TR-3335

9. SPONSORING/MONITORING AGENCY NAME(S) AND ADDRESS(ES)

10. SPONSOR/MONITOR'S ACRONYM(S)

11. SPONSOR/MONITOR'S REPORT NUMBER(S)

12. DISTRIBUTION/AVAILABILITY STATEMENT
Approved for public release; distribution is unlimited.

13. SUPPLEMENTARY NOTES

14. ABSTRACT
Spall strength of a hot-pressed tungsten carbide manufactured by Cercom Inc., referred to as CER-WC, is determined by performing plane shock wave experiments as a function of shock-induced compressive stress and its duration. Shock-induced stress varied between 3.5 and 24 GPa. The duration of shock-induced stress, i.e., pulse width, ranged from 0.35 to 1.13 μs. These experiments showed that CER-WC retained substantial spall strength to 24 GPa, i.e., around 3× the value of the Hugoniot elastic limit. Spall strength of CER-WC was not significantly influenced by the pulse-width of shock-induced compression. Spall strength of CER-WC decreased from a value of 2.06 ± 0.04 to 1.22 ± 0.38 GPa as shock-induced stress increased from 3.4 to 24 GPa.

15. SUBJECT TERMS
shock wave, Hugoniot elastic limit, spall strength, tungsten carbide

16. SECURITY CLASSIFICATION OF:			17. LIMITATION OF ABSTRACT	18. NUMBER OF PAGES	19a. NAME OF RESPONSIBLE PERSON
a. REPORT	b. ABSTRACT	c. THIS PAGE			Dattatraya P. Dandekar
UNCLASSIFIED	UNCLASSIFIED	UNCLASSIFIED	UL	28	19b. TELEPHONE NUMBER (*Include area code*) 410-306-0779

Standard Form 298 (Rev. 8/98)
Prescribed by ANSI Std. Z39.18

Contents

List of Figures

List of Tables

1. Introduction

Tungsten carbide is a high-density ceramic with mechanical properties that make it attractive for applications related to high-velocity impacts. Dandekar and Grady (*1*) report the compressive and shear strengths of a hot-pressed tungsten carbide manufactured by Cercom Inc., referred to as CER-WC, obtained from the results of plane shock wave experiments. This study reports tensile/spall strength of CER-WC obtained from the results of an additional series of plane shock wave experiments, and thus supplements the results reported by Dandekar and Grady (*1*).

Spall strength of ceramic and other brittle materials is generally thought to be controlled by the kinetics of shock-induced defects/damage, i.e., micro- and meso-cracks together with global deformation under a given magnitude of shock-induced stress. Experimentally, spall strength of a ceramic is found to be generally very low, compared to its Hugoniot elastic limit (HEL), and also found to decrease with an increase in shock-induced stress. An exception to this is exhibited by silicon carbide (*2*), in which spall strength is found to increase initially with an increase in the shock-induced stress before the decrease in spall strength with a further increase in shock-induced stress. The goal of the present work was to examine whether or not the duration and amplitude of shock-wave-induced compression had a significant effect on the spall strength of CER-WC, and whether or not the value of spall strength under simultaneous shock-induced compression shear above the HEL of CER-WC more closely resembled that observed in a titanium alloy, Ti-6Al-4V, reported by Spletzer and Dandekar (*3*). The results obtained in this work and those reported in reference (*1*) provide information needed to determine material parameters used in various material models for computational simulations of high-velocity ballistic-impact-induced events.

2. Material

CER-WC is not strictly monolithic, but is composed of two distinct materials, namely WC (97.2% by weight) and W_2C (2.8% by weight) (*4*). WC and W_2C both crystallize in hexagonal form. The theoretical densities of these carbides are 15.7 and 17.2 Mg/m^3, respectively (*4*). Both melt around 3050 K and have similar thermal expansion coefficients. The values of density, elastic longitudinal, and shear wave velocities of this composite are 15.530 ± 0.007 (Mg/m^3), 7.05 ± 0.06 km/s and 4.32 ± 0.04 km/s, respectively. At present, the elastic properties of individual phase in this material are not completely measured. Moreover, the reported values of theoretical densities of WC and W_2C suggest that the composite material must contain some lighter impurities and/or voids. The void/volume fraction in this material is reported to be

around 0.01 (*4*). The grain sizes in CER-WC vary between 0.3 and 1.4 μm, with an average grain size of 0.9 μm.

3. Experimental Methods

Plane shock wave experiments were conducted at the U.S. Army Research Laboratory (ARL) 100-mm light gas gun facility. A typical configuration of shock wave experiments performed on tungsten carbide is shown in figure 1. In these experiments, an impactor, i.e., a thinner disc of CER-WC or c-cut sapphire (S) or x-cut quartz (Q) of appropriate thickness, impacted a relatively thicker CER-WC disc (target) with a given velocity to generate a shock compression wave of a certain magnitude and of known duration (pulse width). The adopted configuration of the experiments assured that the recorded wave profiles in these experiments would yield information pertaining to the HEL, the nature of shock-induced deformation, shear strength, release impedance, and spall strength of the material. The wave velocity profiles in these experiments were monitored at the center of the free-surface of the target by employing the velocity interferometer system for any reflective surface (VISAR), developed by Barker and Hollenbach (*5*). Impact velocities were measured by shorting four electrically-charged pins located at measured distances a few millimeters ahead of the target disc. The planarity of impact was better than 0.5 mrad. The precision of free-surface velocity measurements is 1%. Uncertainties in the measured values of impact velocities are 0.5%. Seventeen spall experiments were performed on CER-WC.

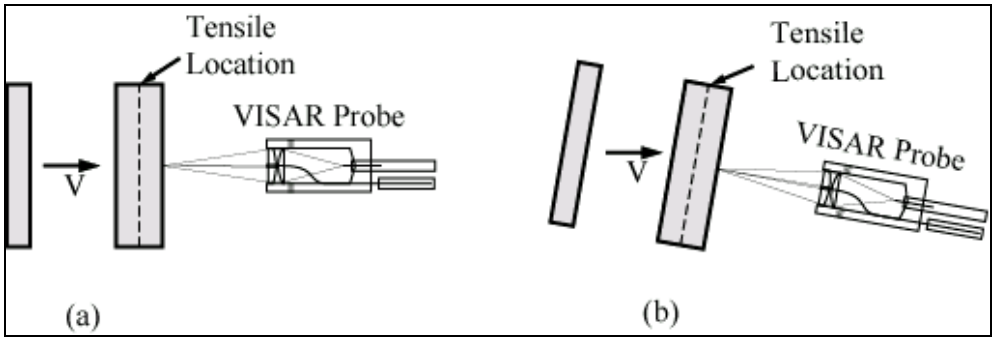

Figure 1. Configuration of shock wave spall experiments: (a) normal impact and (b) compression shear.

4. Results

Tables 1 and 2 summarizes available shock wave compression data on CER-WC, as reported by Dandekar and Grady (*1*), together with such data collected during the course of the present investigation. Table 3 summarizes the spall data obtained from these experiments. Free-surface velocity profiles recorded in spall experiments are shown in figures 2–7.

4.1 Compression and release response

The first cusp in the recorded wave profiles, identified as the HEL, varies from 6.9 to 9.0 GPa. The results of shock wave compression experiments on CER-WC indicated that the HEL varied from 6.2 to 7.6 GPa (*1*). The average value of the HEL, based on all data, was 7.2 ± 0.8 GPa. The observed variation in the values of the HEL is larger than the precision of measurements, i.e., 1.5%. The large statistical uncertainty associated with the average value of the HEL seems to arise from variability of the material itself. For example, in experiments performed at around 23-24 GPa, the values of HEL in targets of nominal thickness of 6 mm vary from 7.34 to 8.96 GPa.

The shock wave following the elastic precursor travels in the elastically-deformed material with velocity varying from 5.1 to 6.2 km/s. These values of inelastic/plastic shock wave velocity exceed the magnitude of bulk sound wave velocity in CER-WC at the ambient condition, i.e., 4.96–4.98 km/s. This suggests that deformation of CER-WC is elastic-plastic. However, the large values of plastic wave velocities obtained in experiments 507, 302-1, and 302-2 are inexplicable. These exceptionally large values are not consistent with the values of plastic velocities obtained in the remaining experiments. The least squares fit to shock velocity and mass velocity data, omitting those obtained in the previously mentioned three experiments yields the following equation:

$$U(P) = 5.088 + 1.419\, u(P), \qquad (1)$$

where U (P) and u (P) are the plastic wave velocity and mass velocity corresponding to inelastic deformation in CER-WC. The correlation coefficient for the relation given by equation 1 is 0.976, and 95% confidence intervals for the intercept and slope are ±0.101 and ±0.237 km/s, respectively. Equation 1 is used to calculate plastic wave velocities in experiments 301-1 and 409.

The inelastic/plastic stresses and densities given in tables 1 and 2 are obtained by using the well-known momentum and mass conservation relations centered at the HEL (*3*).

Table 1. Shock wave compression and release data on CER-WC (according to Dandekar and Grady [*2*]).

Experiment	Impactor Thickness (mm)	Target Thickness (mm)	Impact Velocity (km/s)	Elastic Compression			Plastic Compression				Free-Surface Velocity (km/s)	Release Impedance (Gg/m^2s)
				Stress (GPa)	Mass Velocity (km/s)	Density (Mg/m^3)	Plastic Velocity (km/s)	Stress (GPa)	Mass Velocity (km/s)	Density (Mg/m^3)		
504	3.148	3.137	0.6130	6.793	0.0620	15.678	5.43	27.61	0.3065	16.417	0.5939	96.1
507	2.023 (S)	3.139	0.2962	7.362	0.0672	15.690	5.79	9.28	0.0883	15.747	0.1815	99.5
514-1	2.025 (S)	3.147	0.5067	6.354	0.0580	15.669	5.29	15.24	0.1652	15.993	0.3080	106.7
514-2	3.141	6.429	0.5067	7.559	0.0690	15.694	5.56	23.66	0.2534	16.232	0.4950	97.9
516	0.994 (Q)	6.478	0.5004	6.475	0.0591	15.671	—	—	—	—	0.1183	—
517	3.145	6.476	0.1848	6.847	0.0625	15.679	5.10	9.24	0.0924	15.772	0.1717	116.5
102	4.000	6.000	0.0648	3.495	0.0319	15.611	—	—	—	—	0.0638	—
103	4.000	6.000	0.0644	3.440	0.0314	15.610	—	—	—	—	0.0628	—
WC-8	6.200	6.178	1.6600	6.201	0.0566	15.666	6.22	81.56	0.8300	17.890	—	—
WC-12	1.507 (Al)	6.192	0.3620	4.295	0.0392	15.627	—	—	—	—	—	—
WC-13	1.500 (Al)	6.190	0.4540	5.905	0.0539	15.660	—	—	—	—	—	—
WC-14	6.351	6.342	1.2390	6.201	0.0566	15.666	5.98	58.98	0.6200	17.295	—	—
WC-15	6.354	3.000	1.2100	6.201	0.0566	15.666	5.93	57.15	0.6050	17.262	—	—
WC-16	6.350	6.341	0.8240	6.201	0.0566	15.666	5.74	38.16	0.4120	16.700	—	—

Notes: Impactor material is identified only when it is different from CER-WC. Impactor material is CER-WC unless identified as c-cut sapphire (S), x-cut quartz (Q), or aluminum (Al).

Table 2. Shock wave compression and release data on CER-WC (according to present work).

Experiment	Impactor Thickness (mm)	Target Thickness (mm)	Impact Velocity (km/s)	Elastic Compression			Plastic Compression				Free-Surface Velocity (km/s)	Release Impedance (Gg/m^2s)
				Stress (GPa)	Mass Velocity (km/s)	Density (Mg/m^3)	Plastic Velocity (km/s)	Stress (GPa)	Mass Velocity (km/s)	Density (Mg/m^3)		
301-1	2.020	5.950	0.2000	7.450	0.0680	15.691	5.24	10.10	0.1000	15.78	0.2080	—
302-1	2.030	6.030	0.4047	7.045	0.0643	15.683	5.81	19.62	0.2023	16.065	0.3975	100.5
302-2	3.990	6.030	0.4047	7.045	0.0643	15.683	5.81	19.62	0.2023	16.065	0.4058	96.4
315-1	2.001	6.030	0.1255	6.880	0.0628	15.680	—	—	—	—	0.1298	—
315-2	3.994	6.031	0.1255	6.880	0.0628	15.680	—	—	—	—	—	—
329	2.018	5.965	0.5278	7.340	0.0670	15.689	5.48	24.27	0.2639	16.274	0.4912	106.8
330	3.992	5.971	0.5202	7.340	0.0670	15.689	5.48	23.94	0.2601	16.262	0.4961	101.5
335/CS12º	3.999	6.045	0.5085	8.765	0.0800	15.718	5.51	23.36	0.2486[a]	16.214	0.4665	107.2
401	3.998	6.032	0.5029	8.962	0.0818	15.722	5.52	23.68	0.2514	16.221	0.4800	103.6
407	3.987	6.035	0.1397	7.65	0.0698	15.698	—	—	—	—	—	—
409	3.985	6.042	0.2008	8.89	0.0810	15.724	5.24	10.14	0.1004	15.783	0.1953	—
415/CS12°	3.989	6.044	0.1455	7.79	0.0712[a]	15.702	—	—	—	—	—	—

[a] Mass velocities are half the normal component of impact velocity consistent with 12° obliquity of impact in these experiments.

Table 3. Spall strength of CER-WC.

Experiment	Pulse-width (μs)	Impact stress (GPa)	Free-Surface Velocity (km/s)			Half Pullback Velocity (km/s)			Spall Strength	
			Peak	Spall	Re-Shock	Magnitude	Error (δ)	Percent (δ)	Magnitude (GPa)	Error
103	1.13	3.44	0.0628	0.0252	0.0629	0.01880	0.0003	0.018	2.06	0.04
516	0.35	6.47	0.1183	0.0941	0.1222	0.01210	0.0008	0.062	1.33	0.08
315-1	0.57	6.87	0.1298	0.0996	0.1282	0.01510	0.0008	0.054	1.65	0.09
407	1.13	7.65	0.1357	0.1143	0.1357	0.01070	0.0009	0.083	1.17	0.10
415/CS12°	1.13	7.79	0.1429	0.1251		0.00890	0.0009	0.107	0.97	0.10
Average		**7.20**				**0.0117**	**0.0008**	**0.072**	**1.28**	**0.09**
507	0.36	9.28	0.1815	0.1492	0.1805	0.01615	0.0012	0.073	1.77	0.13
301-1	0.58	10.10	0.2080	0.1840	0.2070	0.01200	0.0014	0.116	1.31	0.15
517	0.86	9.24	0.1717	0.1444	0.1698	0.01365	0.0011	0.082	1.49	0.12
409	1.13	10.14	0.1953	0.1704	0.1953	0.01245	0.0013	0.104	1.36	0.14
Average		**9.69**				**0.01356**	**0.0012**	**0.094**	**1.49**	**0.14**
514-1	0.36	15.24	0.3080	0.2790	0.2959	0.01450	0.0021	0.143	1.59	0.23
302-1	0.58	19.82	0.3907	0.3667	0.3858	0.01200	0.0027	0.223	1.31	0.29
302-2	1.13	19.82	0.3952	0.3746	0.3935	0.01030	0.0027	0.264	1.13	0.30
Average		**19.82**				**0.01115**	**0.0027**	**0.243**	**1.22**	**0.30**
329	0.50	24.41	0.4912	0.4688	0.4830	0.01120	0.0034	0.303	1.23 (0.86)	0.37
330	0.50	24.08	0.4961	0.4725	0.4881	0.01180	0.0034	0.290	1.29 (0.91)	0.38
514-2	0.82	23.66	0.4950	0.4740		0.01050	0.0034	0.326	1.15 (0.81)	0.38
335/CS12°	1.13	23.36	0.4665	0.4465	0.4665	0.01000	0.0032	0.323	1.10 (0.77)	0.35
401	1.13	23.77	0.4800	0.4580	0.4750	0.01100	0.0033	0.302	1.20 (0.85)	0.36
Average		**23.86**				**0.01113**	**0.0033**	**0.309**	**1.22 (0.84)**	**0.38**

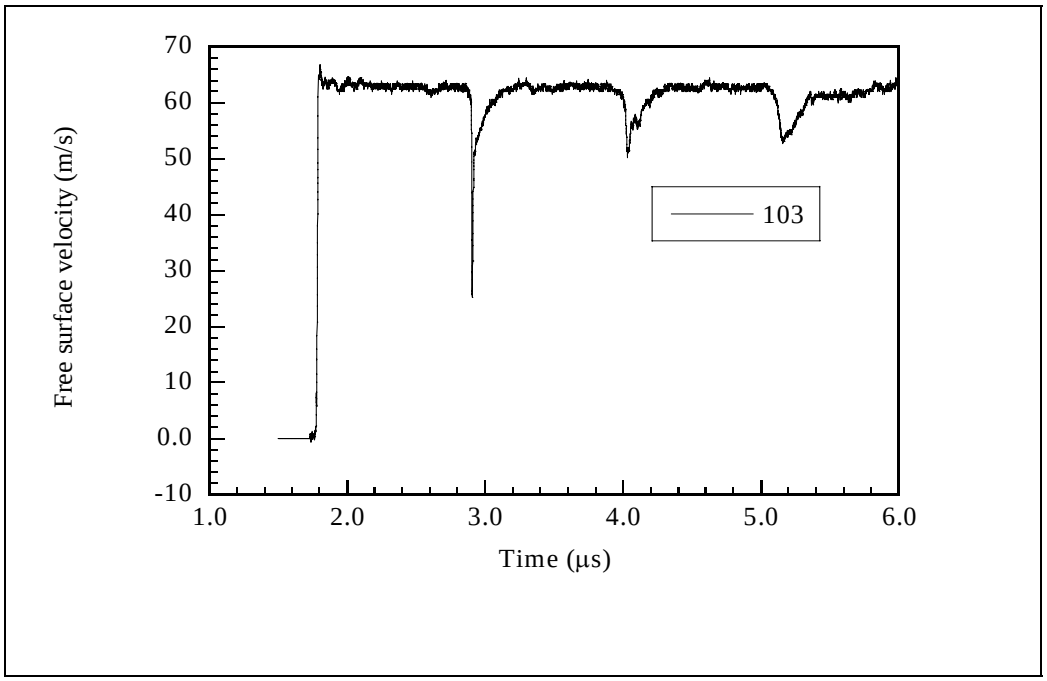

Figure 2. Free-surface velocity profile in CER-WC at 3.4 GPa.

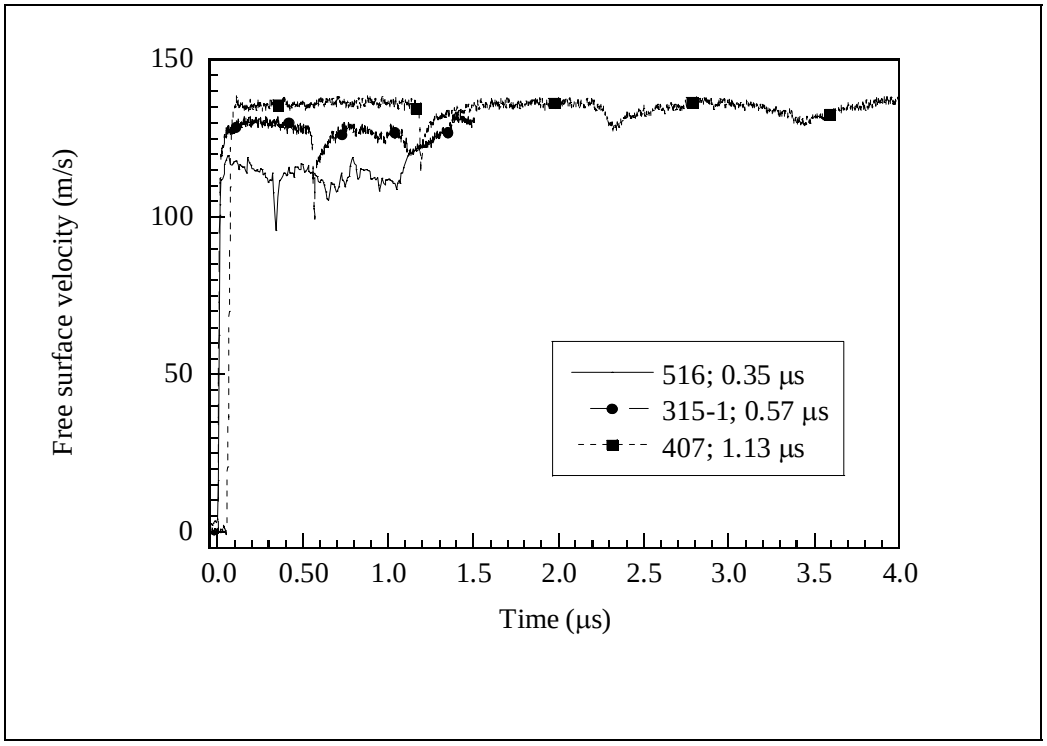

Figure 3. Free-surface velocity profile in CER-WC at 6.5–7.6 GPa.

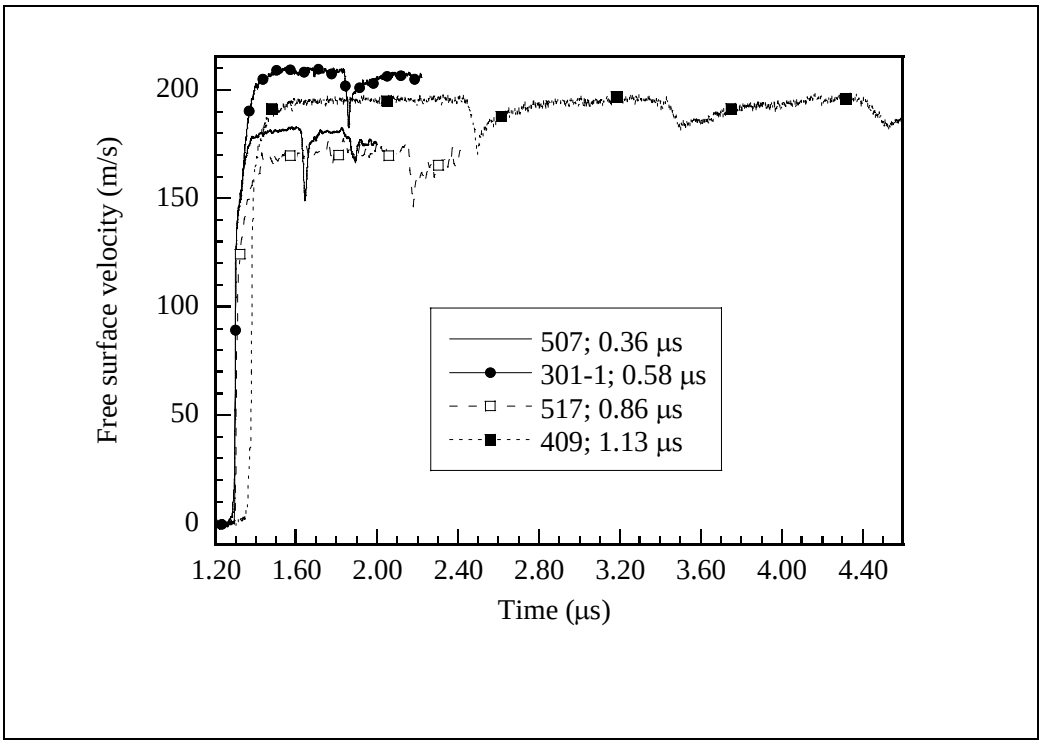

Figure 4. Free-surface velocity profile in CER-WC at 9.2–10.1 GPa.

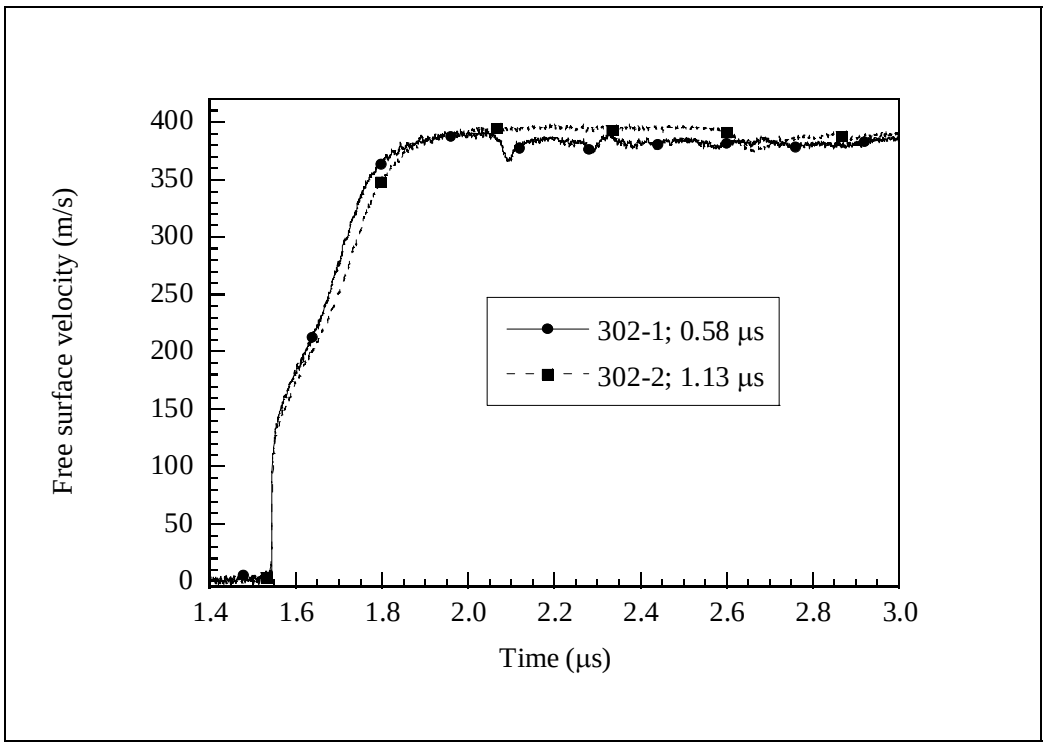

Figure 5. Free-surface velocity profile in CER-WC at 19.8 GPa.

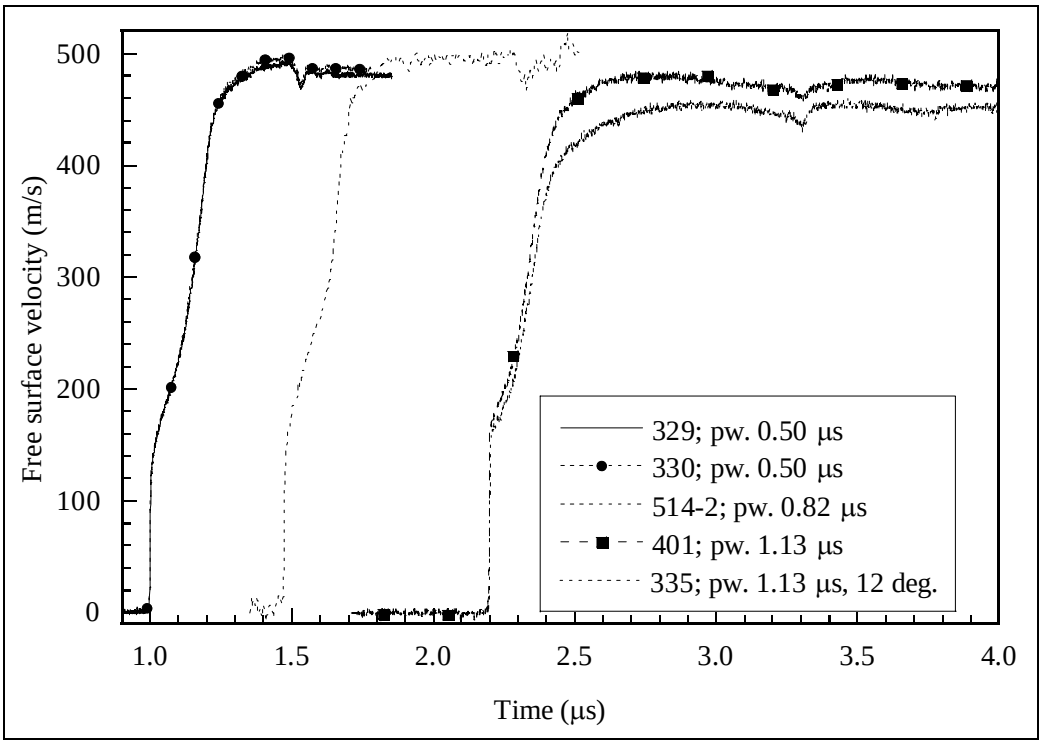

Figure 6. Free-surface velocity profile in CER-WC at 24 GPa.

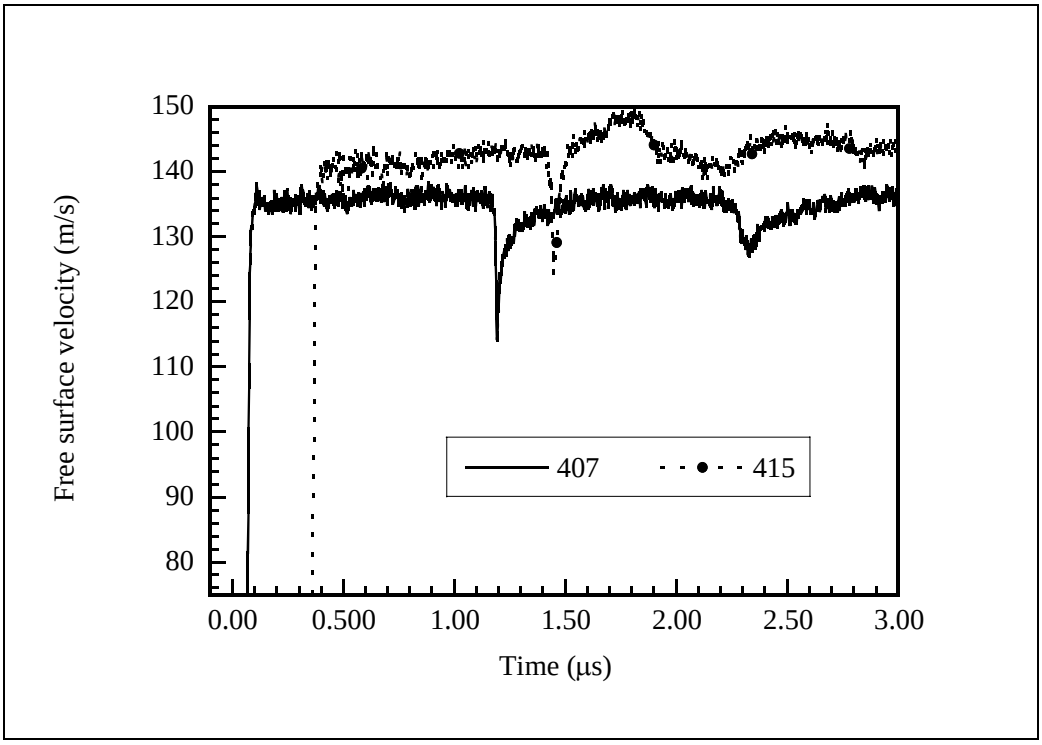

Figure 7. Free-surface velocity profile in CER-WC at 7 GPa under normal and 12° obliquity.

Hydrodynamic compression of CER-WC, reported in reference (*1*), and shock compression data, given in tables 1 and 2, are shown in figure 8. The shock compression data of the present work does not change the general conclusion regarding retention of shear strength in CER-WC under plane shock wave compression reported by Dandekar and Grady (*1*). The values of shear strength tend to increase with an increase in the shock-induced stress in CER-WC. For example, whereas the value of shear strength at the HEL is 2.7 ± 0.3 GPa, its value at 24 and 82 GPa are 3.4 ± 0.3 and 6 ± 0.3 GPa, respectively. However, the work hardening of CER-WC remains to be confirmed through shock-release-re-shock experiments similar to those performed in titanium diboride (*6*).

The effective overall release impedance of CER-WC calculated from the plastic stress, plastic mass velocity, and recorded free-surface velocity range from 96 to 116 Gg/m^{2}s. These values are very close to the elastic impedance of CER-WC, i.e., 109.5 Gg/m^{2}s. This result appears consistent with the work-hardening nature of CER-WC, but needs to be substantiated through the type of experiments suggested in the previous paragraph.

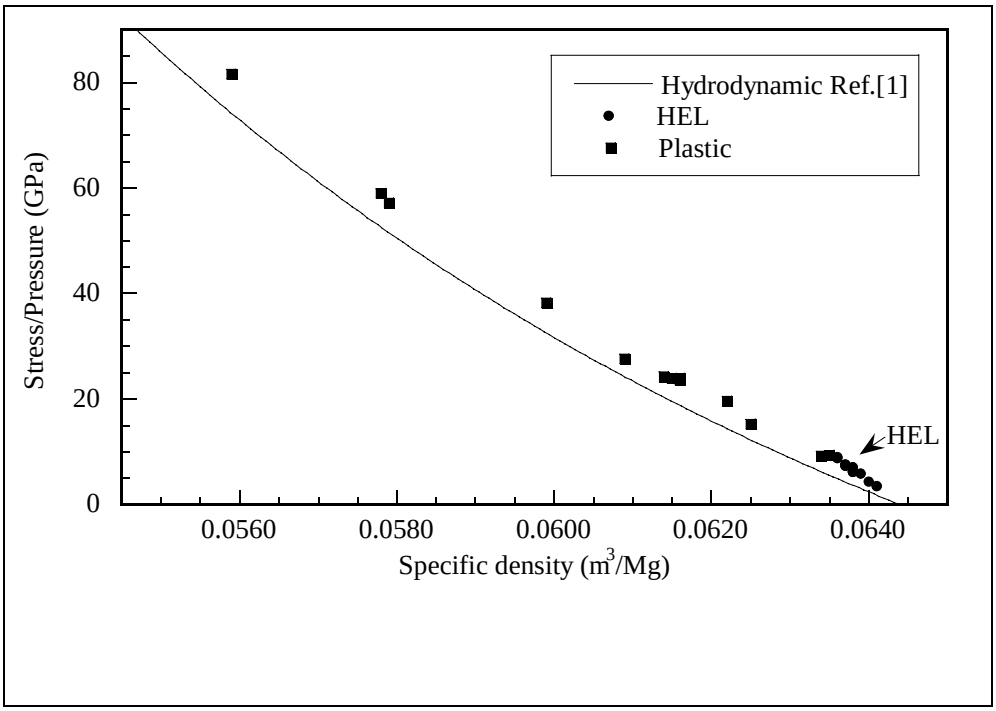

Figure 8. Shock Hugoniot and hydrodynamic compression of CER-WC.

4.2 Spall strength

Table 3 summarizes the spall data and the values of spall strength of CER-WC obtained for various pulse widths at a specific value of impact-induced stress. These experiments were done over a period of years. Thus, the values of spall strengths given in this table provide a measure of variability due to variation in different batches of the CER-WC material. Further, the observations of the variation in the values of spall strength due to pulse width are discussed in

terms of the average impact stresses. It should be noted that in a spall experiment, the free-surface velocities measured from the arrival of a shock compression wave lasts for the duration of the pulse width. Measurements show a precipitous decline in free-surface velocity, indicative of spall, and a recompression wave following the generation of spall in the material. These free-surface velocities are identified as peak, spall, and reshock in table 3. The values of half pull-back velocity given by one-half the product of difference between the peak and spall free-surface is a measure of the spall strength of a material. Based on the assumption that the observed release impedance is elastic, the values of spall strengths are calculated from the product of half pull-back velocity and longitudinal elastic impedance of CER-WC. However, if future experiments show that tensile impedance of CER-WC is plastic, then the more realistic value of spall strength would be less than the values based on elastic impedance. For example, if the tension from an impact stress of 24 GPa is generated following a plastic path, then a lower bound on the spall strength at 24 GPa for CER-WC may be estimated by multiplying the observed half pull-back velocity with the ambient plastic impedance of CER-WC. The ambient plastic impedance is given by the product of the ambient density and bulk sound wave velocity. The value of the ambient plastic impedance of CER-WC is thus 77.2 Gg/ m^2s. These lower values of spall strengths at 24 GPa for CER-WC are given in parenthesis in table 3.

Results of these experiments show that when shocked to 24 GPa, i.e., around 3× the value of the HEL, CER-WC retains substantial spall strength. The observed scatter in the values of pull-back velocity declines with an increase in the impact stress, even though the errors in the measurements increase substantially (table 3). The upper and lower extreme, shown in figure 9, are the maximum and minimum pull-back velocities recorded at given average impact stresses (table 3). The reasons for the observed large scatter at low stresses and reduction in the scatter at high stresses for the pull-back velocity in CER-WC are difficult to state with any confidence due to the paucity of material properties data for WC and W_2C phases in CER-WC, the two phases constituting CER-WC. The measured values of spall strength show an initial large decline of impact stresses from 3.4 to 7 GPa, compared to those from 7 to 24 GPa. Further, the dependence of spall strength of CER-WC on pulse width, i.e., duration of shock-induced compression, is at best moderate and the values of spall strength as indicated by the magnitude of half pull-back velocity are not significantly different above 7 GPa. A relatively large decrease in the spall strength of CER-WC when shocked from 3.4 to 7 GPA and a much smaller gradual decrease in the spall strength of CER-WC from 7 to 24 GPa suggests that weakening due to shock-induced compressive fracture damage is apparently compensated/mitigated through blunting of cracks and propagation due to shock-induced plastic deformation of CER-WC, a dissipative process, initiated at and above stresses around magnitude of the HEL.

Two spall experiments, 335/CS12° and 415/CS12°, were performed under simultaneous compression-shear at 12° obliquity on CER-WC at 23.4 and 7.8 GPa, respectively, to determine the role of induced shear stress under simultaneous compression-shear on the spall strength of CER-WC. The configuration of the experiments assured that the shock-induced shear wave

would traverse the spall plane located at around 2 mm from the impact surface of CER-WC target prior to generation of tension in the target at the spall plane. A space-time diagram for these compression-shear experiments is shown in figure 10. It was expected that, to the extent that the deformation was controlled through shock-induced plasticity, the spall strength of CER-WC would not degrade significantly. The measured value of half pull-back velocity is 0.0100 ± 0.0032 km/s in experiment 335/CS12° and is not significantly different from the measured values of half pull-back velocity 0.0110-0.0118 km/s under normal shock-induced compression, i.e., at 0° obliquity. A similar result is obtained from experiment 415/CS12° at 7.8 GPa. The results of these two experiments appear to be consistent with the idea that plastic deformation of CER-WC mitigates the effect of weakening due to compressive fracture damage through blunting of cracks and their propagation.

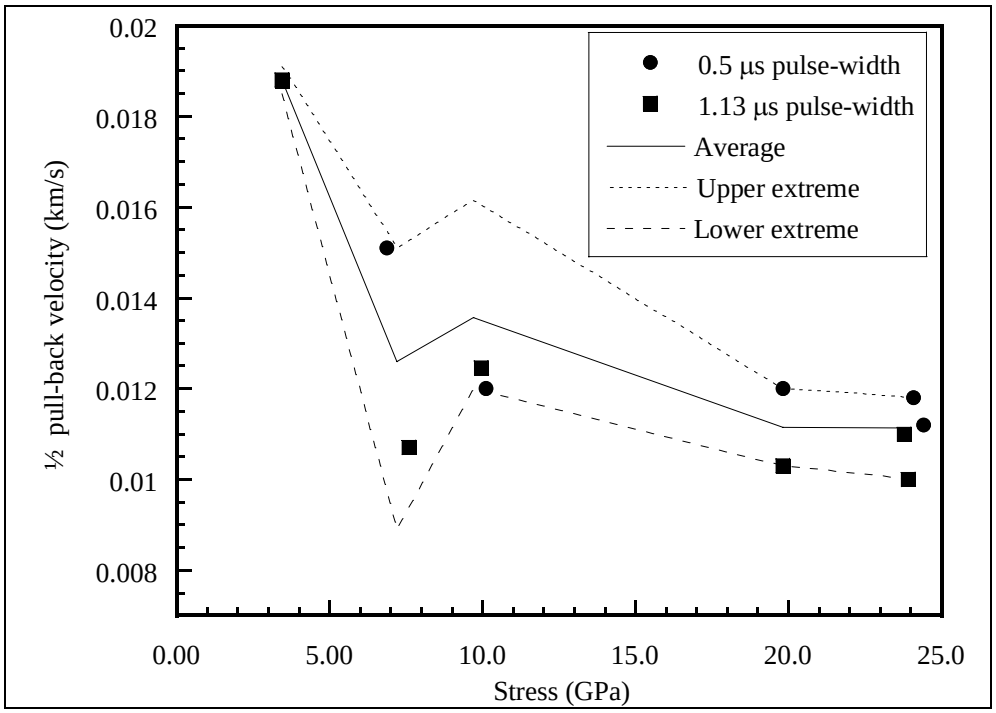

Figure 9. Pull-back velocity as a function of stress and pulse width for CER-WC.

Frutschy et al. (*7*) report the results of pressure-shear experiments on pure WC obtained from Cercom, Inc. at around 6.5 and 19.5 GPa at 18° and 16° obliquities, respectively. The values of density, longitudinal, and shear wave velocities for the pure WC are 15.4 Mg/m^3, 6.86, and 4.3 km/s, respectively. Based on theoretical density of WC, pure WC was reported to have 1.5% porosity. Pure WC was taken to be a single phase material with no metallic additive. But pure WC material provided to them for their investigation by ARL was CER-WC. Thus, the values of density, elastic wave velocities, and porosity should be those given in section 2. They found that the normal velocity component wave profiles show features similar to those observed in free-surface velocity profiles under normal plane shock wave loading to 8 and 20 GPa. The values of 8 and 20 GPa are based on the results of shock wave experiments given in tables 1 and 2. But

the free-surface velocity profiles corresponding/related to shear wave velocity component in these two experiments displayed different patterns. Whereas the free-surface velocity profiles corresponding/related to shear wave velocity component at lower peak stress, i.e., 8 GPa, rose to stable value within a duration of around 0.2 μs, the profile at 20 GPa showed a ramp-like structure and rose slowly to a stable magnitude over a duration of 0.7 μs. The peak magnitudes of shear stress-induced free-surface velocity in these two experiments were 0.04 and 0.138 km/s, respectively. They attributed the recorded ramp-like shear wave front at 20 GPa to dissipative frictional processes associated with the damage resulting from collapse of pores initially present in the pure WC. Since the porosity in CER-WC is estimated to be around 1%, the relative role of dissipative effects of plasticity and pore collapse on the observed spall strength of CER-WC under simultaneous compression-shear and under pure compression under shock wave loading remains to be determined. However, based on almost exact matching of normal velocity wave profiles under compression alone and under compression-shear at 7 and 23 GPa, respectively (see figure 6 profiles for experiments 401 and 335 and figure 7 profiles for experiments 407 and 415), suggests that spall strength itself may not be influenced significantly due to the dissipative frictional processes associated with collapse of pores as manifested in the shear wave velocity profiles. It would be fruitful to conduct pressure-shear experiments on CER-WC to higher magnitudes of compressive stress.

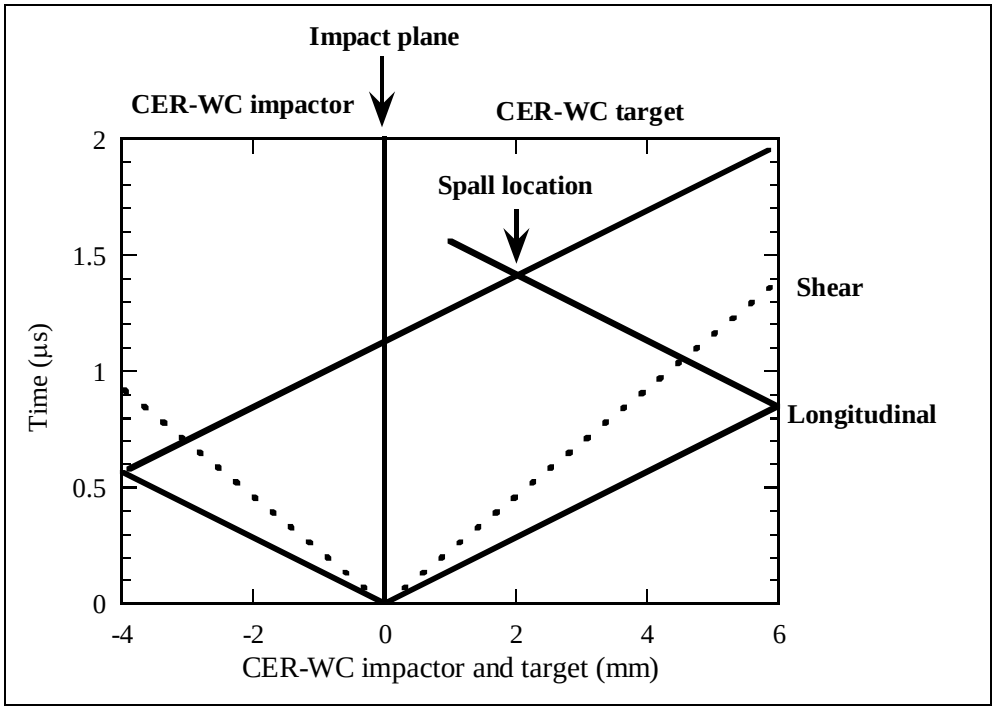

Figure 10. X-t diagram of simultaneous compression-shear spall experiments in CER-WC.

The results of spall experiments under normal impact and under simultaneous compression-shear show that the measured values of half pull-back velocity are not significantly different from one another. It remains necessary to perform additional spall experiments under simultaneous

compression-shear both below and above the HEL of CER-WC to strengthen the previously mentioned suggestion of a mitigating effect of plastic deformation on cracks/damage. Finally, the magnitudes of spall strength expressed in terms of stress to 20 GPa would show a sudden decline in its value at 24 GPa if the effective tensile impedance at 24 GPa is plastic. For example, the spall strength of CER-WC would decrease from a value of 2.06–1.22 GPa as shock-induced stress increased from 3.44 to 19.82 GPa. The value of spall strength of CER-WC at 24 GPa is 1.22 GPa if the effective tensile impedance is elastic. On the other hand, if the effective tensile impedance of CER-WC is plastic, then the magnitude of spall strength becomes 0.84 GPa for the same value of the observed half pull-back velocity at 24 GPa. This is an expected response, since at 24 GPa tension may be generated through interaction of release waves in CER-WC following plastic loci, as was indeed the case for a heavy tungsten alloy 93W. Dandekar and Weisgerber (*8*) measured values of tensile impedance for 93W, deforming like an elastic-plastic material under shock wave propagation, in spall experiments where tensile stresses were generated through interaction of release waves following plastic loci. The values of tensile impedance were indeed close to the value of the plastic impedance of 93W. Grady (*9*) reported spall strength of CER-WC at impact stresses of 4.3 and 5.9 GPa to be 1.65 ± 0.05 and 1.4 ± 0.1 GPa, respectively. These values are consistent with the measured values of spall strength of CER-WC obtained at 3.4 and 7 GPa.

Finally, the quasi-static tensile strength of CER-WC is reported to be 0.59 ± 0.06 GPa (*4*). This large difference in the spall strength of CER-WC, measured quasi-statically and under plane shock wave loading, can be due to differences in the stress and strain states, and strain rates under uniaxial stress state attained under quasi-static loading condition and uniaxial strain state achieved under plane shock wave propagation. Strain rates control kinetics and the time available determines the generation and propagation of defects. Bridgman (*10*) measured tensile strengths of brittle and ductile materials under hydrostatic pressure. In general, he found that tensile strengths of materials increased significantly under high hydrostatic pressures. For example, the tensile strength of carboloy, a tungsten carbide cermet containing metallic cobalt binder, increased by two to three times under hydrostatic pressure of 2.6 GPa compared to under the ambient pressure. Thus, the measured lower magnitude of quasi-static spall strength 0.59 ± 0.06 GPa of CER-WC is at least in part due to the unconfined loading condition. Since spall strength measurements of a material under plane shock wave loading is done under the uniaxial strain condition, i.e., a confined condition, the smaller magnitude of quasi-static tensile strength of CER-WC compared to its spall strength is consistent.

5. Summary

1. Shock-induced compression and release response of CER-WC may be modeled as an elastic-plastic solid material to 82 GPa. The HEL of CER-WC is 7.2 ± 0.8 GPa.

2. Shear strength of CER-WC increases with an increase in the shock-induced stress to 82 GPa. The values of shear strength at the HEL and at 82 GPa are 2.7 ± 0.3 and 6.0 ± 0.3 GPa, respectively.

3. The effective release impedance of CER-WC to 24 GPa is elastic.

4. Spall strength of CER-WC decreases with an increase in the shock-induced compressive stress. It does not show a strong dependence on duration/pulse-width of shock-induced compressive stress between 0.5 and 1.1 μs. The initial decline in spall strength is very rapid, decreasing from a value of 2.06 ± 0.08 to 1.38 ± 0.12 GPa when shocked to 3.4 and 7.2 GPa, respectively. An increase in the shock stress to 24 GPa leads to only a moderate decrease in the value of spall strength at 24 GPa, i.e., 1.22 ± 0.45 GPa. A lower bound of the magnitude of spall strength, based on plastic impedance of CER-WC at 24 GPa, is 0.84 ± 0.31 GPa.

5. The mitigation of the initial precipitous decline in the spall strength of CER-WC appears to be due to the mitigating influence of plasticity-dominated deformation on compressive stress-induced damage in CER-WC, i.e., blunting of cracks or microcracks above the HEL. However, the role and contributions of pore collapse suggested by Frutschy et al. (*7*), and the deformation of WC and W_2C phases under shock wave compression and simultaneous compression-shear on the spall strength of CER-WC, although unknown, cannot be discounted to understand the spallation of CER-WC.

6. Finally, quasi-static tensile strength of CER-WC is reported to be 0.59 ± 0.06 GPa, significantly less than the spall strength of the material determined in this study showing the combined influences of kinetics of defect generation and confined stress state of CER-WC on the value of its spall strength.

6. References

1. Dandekar, D. P.; Grady, D. E. Shock Equation of State and Dynamic Strength of Tungsten Carbide. *Shock Compression of Condensed Matter—2001*; Furnish, M. D., Thadhani, N. N., Horie, Y., Eds.; American Institute of Physics: NY, 2002; pp 783–786.

2. Dandekar, D. P.; Bartkowski, P. T. Spall Strengths of Silicon Carbides Under Shock Loading. *Shock Wave and High-Strain Rate Phenomena;* Staudhammer, K. P., Murr, L. E., Meyers, M. A., Eds.; Elsevier: NY, 2001; pp 71–77.

3. Spletzer, S. V.; Dandekar, D. P. *Deformation of a Low-Cost Ti-6Al-4V Armor Alloy Under Shock Loading*; ARL-TR-2386, U.S. Army Research Laboratory: Aberdeen Proving Ground, MD, 2001.

4. Gooch, W. A.; Burkins, M. S.; Palicka, R. Ballistic Development of U. S. High Density Tungsten Carbide Ceramics. *J. de Physique IV* **2000**, *10*, 735–741.

5. Barker, L. M.; Hollenbach, R. E. Laser Interferometer for Measuring High Velocities of any Reflecting Surface. *J. Appl. Phys.* **1972,** *43*, 4669–4675.

6. Dandekar, D. P. Response of Protective Ceramics Under Single and Multiple Impacts. *Wave Propagation and Emerging Technologies*, AMD-Vol. 188; Kinra, V. K., Clifton, R. J., Johnson, G. C., Eds.; ASME Press: NY, 1994; pp 133–141.

7. Frutschy, K. J.; Clifton, R. J.; Mello, M. High Temperature Pressure Shear Plate Impact Studies on OFHC Copper and Pure WC. *Shock Compression of Condensed Matter-1997*; Schmidt, S. C., Dandekar, D. P., Forbes, J. W., Eds.; American Institute of Physics: NY, 1998, pp 463–466.

8. Dandekar, D. P.; Weisgerber, W. J. Shock Response of a Heavy Tungsten Alloy. *Int. J. of Plasticity* **1999**, *15*, 1291–1309.

9. Grady, D. E. Private communication, 1996.

10. Bridgman, P. W. *Studies in Large Plastic Flow and Fracture*; Harvard: Cambridge, 1964; pp. 106–11.

NO. OF COPIES ORGANIZATION

1 (PDF ONLY) DEFENSE TECHNICAL INFORMATION CTR
DTIC OCA
8725 JOHN J KINGMAN RD
STE 0944
FT BELVOIR VA 22060-6218

1 COMMANDING GENERAL
US ARMY MATERIEL CMD
AMCRDA TF
5001 EISENHOWER AVE
ALEXANDRIA VA 22333-0001

1 INST FOR ADVNCD TCHNLGY
THE UNIV OF TEXAS
AT AUSTIN
3925 W BRAKER LN STE 400
AUSTIN TX 78759-5316

1 US MILITARY ACADEMY
MATH SCI CTR EXCELLENCE
MADN MATH
THAYER HALL
WEST POINT NY 10996-1786

1 DIRECTOR
US ARMY RESEARCH LAB
IMNE AD IM DR
2800 POWDER MILL RD
ADELPHI MD 20783-1197

3 DIRECTOR
US ARMY RESEARCH LAB
AMSRD ARL CI OK TL
2800 POWDER MILL RD
ADELPHI MD 20783-1197

3 DIRECTOR
US ARMY RESEARCH LAB
AMSRD ARL CS IS T
2800 POWDER MILL RD
ADELPHI MD 20783-1197

NO. OF COPIES ORGANIZATION

ABERDEEN PROVING GROUND

1 DIR USARL
AMSRD ARL CI OK TP (BLDG 4600)

NO. OF COPIES ORGANIZATION

1 CECOM
SP & TRRSTRL COMMCTN DIV
AMSEL RD ST MC M
H SOICHER
FT MONMOUTH NJ 07703-5203

1 PRIN DPTY FOR TCHNLGY HQ
US ARMY MATCOM
AMCDCGT
R PRICE
5001 EISENHOWER AVE
ALEXANDRIA VA 22333-0001

1 PRIN DPTY FOR ACQUSTN HQS
US ARMY MATCOM
AMCDCGA
D ADAMS
5001 EISENHOWER AVE
ALEXANDRIA VA 22333-00001

1 DPTY CG FOR RDE HQS
US ARMY MATCOM
AMCRD
5001 EISENHOWER AVE
ALEXANDRIA VA 22333-00001

1 ASST DPTY CG FOR RDE HQS
US ARMY MATCOM
AMCRD
COL S MANESS
5001 EISENHOWER AVE
ALEXANDRIA VA 22333-00001

3 AIR FORCE ARMAMENT LAB
AFATL DLJW
W COOK
D BELK
J FOSTER
EGLIN AFB FL 32542

1 DPTY ASSIST SCY FOR R & T
SARD TT
THE PENTAGON RM 3E479
WASHINGTON DC 20310-0103

1 DARPA
L STOTTS
3701 N FAIRFAX DR
ARLINGTON VA 22203-1714

NO. OF COPIES ORGANIZATION

1 DIRECTOR
US ARMY RESEARCH LAB
AMSRL CS AL TA
2800 POWDER MILL ROAD
ADELPHI MD 20783-1145

3 DIRECTOR
US ARMY ARDEC
AMSTA AR FSA E
W P DUNN
J PEARSON
E BAKER
PICATINNY ARSENAL NJ
07806-5000

2 US ARMY TARDEC
AMSTRA TR R MS 263
K BISHNOI
D TEMPLETON
WARREN MI 48397-5000

3 COMMANDER
US ARMY BELVOIR RD&E CTR
STRBE N WESTLICH
STRBE NAN
S G BISHOP
J WILLIAMS
FORT BELVOIR VA 22060-5166

1 COMMANDER
US ARMY RESEARCH OFFICE
A RAJENDRAN
PO BOX 12211
RESEARCH TRIANGLE PARK NC
27709-2211

1 NAVAL RESEARCH LAB
A E WILLIAMS
CODE 6684
4555 OVERLOOK AVE SW
WASHINGTON DC 20375

6 DIRECTOR
LANL
P MAUDLIN
R GRAY
W R THISSELL
A ZUREK
Y HORIE
F ADDESSIO
PO BOX 1663
LOS ALAMOS NM 87545

NO. OF COPIES ORGANIZATION

7 DIRECTOR
SANDIA NATL LABS
E S HERTEL JR MS 0819
W REINHART
T VOLGER
R BRANNON MS 0820
L CHHABILDAS MS 1811
M FURNISH MS 0821
M KIPP MS 0820
PO BOX 5800
ALBUQUERQUE NM 87185-0307

2 DIRECTOR
LLNL
J AKELLA
N C HOLMES
PO BOX 808
LIVERMORE CA 94550

2 CALTECH
PROF G RAVICHANDRAN
T J AHRENS MS 252 21
1201 E CALIFORNIA BLVD
PASADENA CA 91125

2 ARMY HIGH PERFORMANCE
COMPUTING RSRCH CTR
T HOLMQUIST
G JOHNSON
1200 WASHINGTON AVE S
MINNEAPOLIS MN 55415

3 SOUTHWEST RESEARCH
INSTITUTE
C ANDERSON
J WALKER
K DANNEMANN
PO DRAWER 28510
SAN ANTONIO TX 78284

2 UNIVERSITY OF DELAWARE
DEPT OF MECH ENGINEERING
PROF J GILLESPIE
NEWARK DE 19716

3 SRI INTERNATIONAL
D CURRAN
D SHOCKEY
R KLOPP
333 RAVENSWOOD AVE
MENLO PARK CA 94025

NO. OF COPIES ORGANIZATION

1 VIRGINIA POLYTECHNIC INST
COLLEGE OF ENGINEERING
R BATRA
BLACKSBURG VA 24061-0219

1 COMPUTATIONAL MECHANICS
CONSULTANTS
JA ZUKAS
PO BOX 11314
BALTIMORE MD 21239-0314

1 KAMAN SCIENCES CORP
D L JONES
2560 HUNTINGTON AVE STE 200
ALEXANDRIA VA 22303

6 INST OF ADVANCED TECH
UNIVERSITY OF TX AUSTIN
S BLESS
H FAIR
D LITTLEFIELD
C PERSAD
P SULLIVAN
S SATAPATHY
3925 W BRAKER LN STE 400
AUSTIN TX 78759-5316

1 APPLIED RSCH ASSOCIATES
D E GRADY
4300 SAN MATEO BLVD NE
STE A220
ALBUQUERQUE NM 87110

1 INTERNATIONAL RESEARCH
ASSOCIATES INC
D L ORPHAL
4450 BLACK AVE
PLEASANTON CA 94566

1 THE DOW CHEMICAL CO
CENTRAL RSRCH ENGINEERING
LABORATORY
M EL RAHEB
BUILDING 1776
MIDLAND MI 48640

1 BOB SKAGGS CONSULTANT
S R SKAGGS
79 COUNTY RD 117 SOUTH
SANTA FE NM 87501

NO. OF COPIES ORGANIZATION

1 WASHINGTON ST UNIVERSITY
SCHOOL OF MECHANCIAL
AND MATERIAL ENGINEERING
J L DING
PULLMAN WA 99164-2920

2 WASHINGTON ST UNIVERSITY
INSTITUTE OF SHOCK PHYSICS
Y M GUPTA
J ASAY
PULLMAN WA 99164-2814

1 COORS CERAMIC COMPANY
T RILEY
600 NINTH ST
GOLDEN CO 80401

1 ARIZONA STATE UNIVERSITY
MECHANICAL AND AEROSPACE
ENGINEERING
D KRAVCINOVIC
TEMPE AZ 85287-6106

1 UNIVERSITY OF DAYTON
RESEARCH INSTITUTE
N S BRAR
300 COLLEGE PARK
MS SPC 1911
DAYTON OH 45469

5 DIRECTOR
USARL
K WILSON (5 CPS)
FRENCH DEA 1396
ADELPHI MD 20783-1197

ABERDEEN PROVING GROUND

54 DIR USARL
AMSRD WM
E SCHMIDT
T WRIGHT
J MACAULEY
AMSRD WM MB
G GAZONAS
J LASALVIA
P PATEL
AMSRL WM TA
P BARTKOWSKI
W A GOOCH
M ZOLTOSKI
E HORWATH
M NORMANDIA
AMSRL WM TC
R COATES

NO. OF COPIES ORGANIZATION

K KIMSEY
D SCHEFFLER
AMSRL WM TD
S SEGELETES
D DANDEKAR (30 CPS)
K IYER
M GREENFIELD
J CLAYTON
H W MEYER
E RAPACKI
S SCHOENFELD
T BJERKE
M SCHEIDLER
T WEERASOORIYA

NO. OF COPIES ORGANIZATION

1 DERA
N J LYNCH
WEAPONS SYSTEMS
BUILDING A20
DRA FORT HALSTEAD
SEVENOAKS
KENT TN 147BP
UNITED KINGDOM

2 ERNST MACH INTITUT
VOLKER HOHLER
H NAHAME
ECKERSTRASSE 4
D 7800 FREIBURG 1 BR 791 4
GERMANY

1 FOA2
P LUNDBERG
S 14725 TUMBA
SWEDEN

1 PCS GROUP
CAVENDISH LABORATORY
W G PROUD
MADINGLEY RD
CAMBRIDGE
UNITED KINGDOM

1 CENTRE D ETUDES DE GRAMAT
J Y TRANCHET
46500 GRAMAT
FRANCE

1 MINISTERE DE LA DEFENSE
DR G BRAULT
DGA DSP STTC
4 RUE DE LA PORTE DISSY
75015 PARIS
FRANCE

1 SPART DIRECTION BP 19
DR E WARINGHAM
10 PLACE GEORGES
CLEMENCEOUX
92211 SAINT CLOUD CEDEX
FRANCE

NO. OF COPIES ORGANIZATION

1 ROYAL MILITARY COLLEGE OF
SCIENCE
CRANEFIELD UNIVERSITY
PROF N BOURNE
J MILLETT
SHRIVENHAM SWINDON
SN6 8LA
UNITED KINGDOM

1 BEN GURIAN UNIVERSITY OF NEGEV
E ZERETSKY
DEPT OF MECH ENG, BEER-SHEVA
ISRAEL 84105

2 RUSSIAN ACADEMY OF SCIENCES
INSTITUTE FOR HIGH ENERGY
DENSITIES
G I KANEL
S V RAZORENOV
IVTAN IZHORSKAYA 13/19
MOSCOW 127412 RUSSIA

INTENTIONALLY LEFT BLANK.